cement-sand injections, chemical injections, subsurface drainage systems, and even minor relocations of the roadbed were considered. The salient point of all the methods considered was that the work of correction had to be performed under railroad traffic conditions.

CONCLUSION

Geotechnical evaluation of a track structure is to be done on a segment basis. Of the phases and activities of a geotechnical evaluation program, the field observation phase and the log of inspection activity are critical. The track cross-trench exploration tool is the most revealing method.

Collection and organization of a geologic data base is important to a continuing program of track support improvement. Laboratory testing procedures must be directed at specific track performance characteristics. Geotechnical solutions to mass earth movements may be necessary to keep a segment of track open for service; however, geotechnical solutions that address day-to-day track maintenance problems are of increasing importance. These latter problems and their solutions are subtle.

Publication of this paper sponsored by Committee on Track Structure Systems Design.

Constitutive Modeling of Materials in Track Support Structures

C.S. DESAI AND R. JANARDHANAM

Track support structures for railroads and other mass transportation vehicles consist of multicomponent systems. Traditionally, the rail-track support bed includes the rail or guideway, ties, ballast, subballast, and the natural ground or subgrade. Under repeated applications of wheel loads from the vehicles the bed is subjected to complex loading conditions. Furthermore, the materials in the bed and their interactions are complex from a physical viewpoint. Hence, appropriate and comprehensive tests are necessary to define the constitutive or stress-strain behavior of these materials. Advanced testing devices with sophisticated and highly sensitive loading systems and deformation detecting systems are used in this study to perform a number of tests on various materials. These include subgrade soil, subballast, ballast, and wood tie, which are tested by using two truly triaxial or multiaxial testing devices. The tests are performed under different stress paths and densities relevant to the site conditions at the UMTA test section, Transportation Test Center (TTC), Pueblo, Colorado. The materials are subjected to a number of load-unload-reload cycles, and the stress-strain responses are recorded. The responses of the materials are examined carefully and appropriate constitutive laws are developed. A critical state, modified cam clay model is found to simulate behavior of the subgrade soil. Although behavior of the subballast is found to be nonassociative, an elastic-plastic hardening model based on the associative rule is proposed as an approximation. A conventional resilient modulus approach is used for the ballast. A variable moduli model is also proposed as an alternative to account approximately for the inelastic behavior of the ballast. Wood is modeled as an orthotropic elastic material. The foregoing models are cast in forms that can be implemented in solution techniques such as the finite-element procedures. Most of the results reported here can be considered new in the sense that the behavior of the materials in track support structures has been studied perhaps for the first time by using the truly triaxial device in which the field conditions can be simulated and materials can be subjected to three-dimensional stress states. The constitutive models are verified with respect to laboratory tests as well as by implementing them in finite-element procedures. The main objective of this paper is to describe the testing and modeling aspects; the implementation aspect is stated only briefly.

The need for development of mass transportation is acute in this country. Considerable attention is being given to improving the existing railroad systems and to planning and rationalizing the design of new rail track beds to suit the needs of high-speed vehicles. For a complete understanding of the behavior of track support structures, the characteristics of various components of the track beds and their behavior under repetitive loads must be determined.

About 40 percent of the funds spent for the upkeep of track beds in North America is spent on the procurement, distribution, and rehabilitation of ballast (1). About 15 to 20 percent is spent to replace decayed ties and repair spike-torn ties (2). Therefore, the identification of failure and other useful criteria of the materials in the track beds and the relationships between loading environment and foundation material behavior will not only make the analysis of track beds more rational and realistic but can also curtail the maintenance cost.

Furthermore, when numerical schemes such as the finite-element method are used to analyze the track bed, the ultimate effectiveness of the high degree of precision and reliability of this method can be achieved only by the use of valid constitutive relations for the materials under consideration. The accuracy and precision of these relations are governed by the applicability of the constitutive law and the ability to measure true material response in the laboratory. Also, evaluation of the material response under laboratory conditions that simulate the field conditions is highly desirable.

The materials in the track bed are subjected to general three-dimensional states of stress. The loads are repetitive and arise from the wheel loads during travel of a single train. The repetitive loads also arise from the passage of a number of trains over a given section of the track. Thus, the track bed is subjected to a series of loading, unloading, and reloading cycles (3).

Conventional laboratory test equipment is not capable of providing the material parameters that account for the effects of three-dimensional stress fields. Therefore, two truly triaxial testing devices have been used in this investigation. A high-capacity, truly triaxial device of 20,000 psi capacity with a sensitive electrical inductance-type deformation detecting system (4) has been used for multiaxial testing of wood tie and ballast. Subgrade soil and subballast have been tested in a 250 psi capacity multiaxial testing device (5).

The objective of this paper is to present descriptions of testing and constitutive models of

Figure 1. View of high-capacity truly triaxial device (1-20,000 psi).

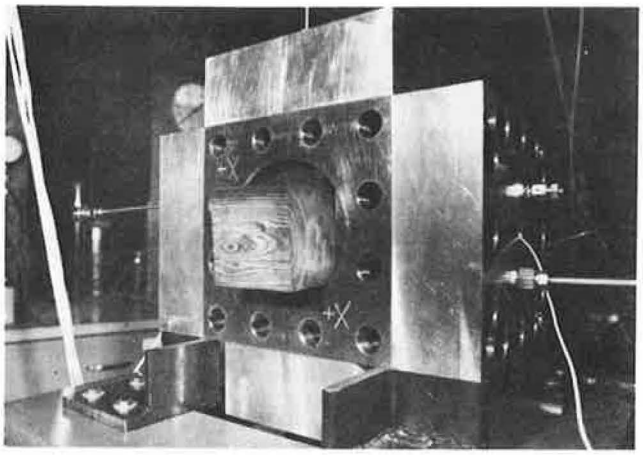

Figure 2. View of low-capacity truly triaxial device (1-250 psi).

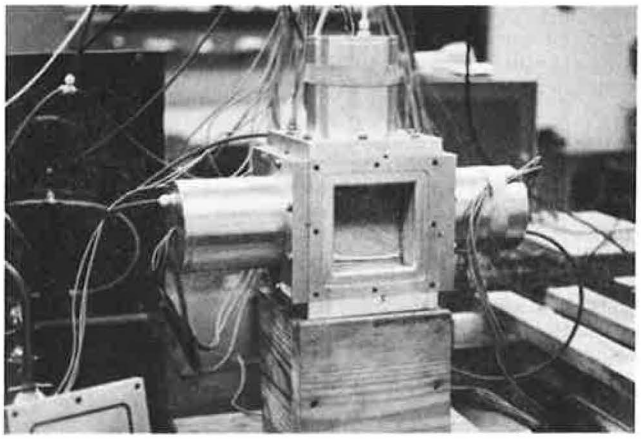

soil, subballast, ballast, and wood tie. In view of space limitations, only brief details and review are presented; additional information is available elsewhere (6-9). The observed stress-strain responses in terms of a series of loading-unloading-reloading cycles under slow or static repeated load are used to obtain appropriate models for different materials.

DETAILS OF MATERIALS TESTED

All the materials tested in this investigation are from UMTA test section at the Transportation Test Center (TTC), Pueblo, Colorado.

Soil

The samples of silty sand in the subgrade of the test section have a specific gravity of about 2.59 with a uniformity coefficient equal to 3.2. The samples are classed as gap-graded material (6). The remolded samples are prepared at its optimum moisture content of 9.1 percent and the maximum dry density of 127.92 lb/ft^3, which are relevant to the site conditions. The initial void ratio of the soil is 0.34.

Subballast

The subballast is a uniformly graded granite gneiss with uniformity coefficient of 1.20. The mean particle size is 1.18 in. With the 4.00-in. cube size specimen permitted in the truly triaxial device, a sample that has large particle size of the field ballast is only tested with difficulty. Hence, the size of the field material is scaled down to two smaller sizes. The technique used is that proposed by Lowe (10), which involves development of the grain size distribution of the test material parallel to that of the field material. The mean grain sizes of the two scaled-down materials are 0.63 and 0.275 in., respectively. The influence of the gradation on strength and deformation properties is also investigated in this study.

Wood Tie

Samples of creosote-coated wood ties used at the UMTA test section are tested. Samples are cut from ties that are free from splits, plate-cut, spike-kill, and shatter. Cut specimens are wrapped in polyethylene sheets and stored in a humidity chamber. The overall average moisture content of the samples is 5.7 percent and the density is 53.00 lb/ft^3.

TESTING PROGRAM

Truly Triaxial Device

The truly triaxial devices [Figures 1 (4) and 2 (5)] used are capable of applying homogeneous and independently controlled three-dimensional stress state on 4.00- x 4.00-in. cubical specimens through flexible membranes. A cubical specimen made from the material of desired density is inserted in the cubical cavity of the frame. In the high-capacity cell the load is applied on each face through an assembly of flexible pads and hydraulically pressurized membrane. In the low-capacity device the load is applied through thin flexible membranes and compressed air is used to apply the pressure. Both devices are stress controlled; further details are given elsewhere (4,5).

Sample Preparation

A special sample preparation mold made of four thin aluminum plates of 4.00 x 4.00 x 0.25 in. is used for preparing samples of soil, subballast, and ballast. The material is spooned into the mold that sits on a base plate and then compacted either by vibration or tamping. The shape and size of the specimen are maintained by applying vacuum pressure through a thin Teflon tube, one end of which is buried in the bed of the material. The mold is removed carefully and the sample is inserted in the apparatus through the side of the cell frame by using a thin lubricated Plexiglas sheet as a ramp. After all the walls are fixed to the frame an initial confining pressure commensurate with the vacuum pressure on the sample is applied, and then the vacuum pressure is disconnected. The sample is then tested along the desired stress path.

Samples of wood are cut from ties and then trimmed to the size of 4.00-in. cube and holes, if any, on the faces of the samples are plugged with plastic putty. The specimens cut are of two kinds (a) with $\alpha = 0$ degrees, where α = inclination of longitudinal grains with a horizontal plane, and (b) with $\alpha = 45$ degrees.

Testing

Tests are conducted on the soil, subballast, and ballast by following a number of significant stress

Figure 3. Commonly used stress paths.

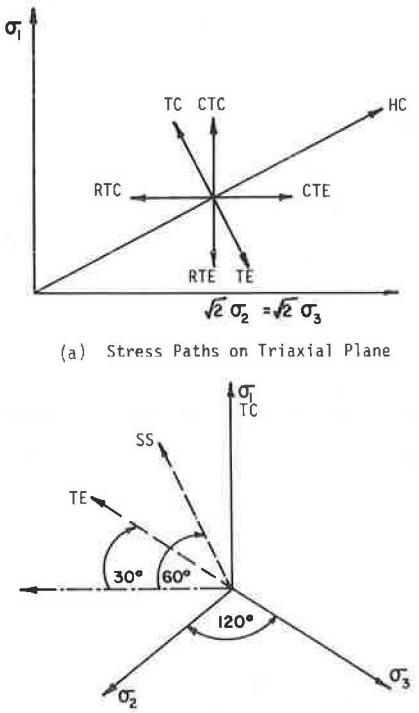

(a) Stress Paths on Triaxial Plane

(b) Stress Paths on the Octahedral Plane

paths (Figure 3). Loads (stresses) are applied on the six faces of the sample. The stresses on the opposite faces are the same. The resulting deformations are recorded after each increment of load is applied and stabilized as the particular stress path is followed. Wooden samples are also tested following different stress paths; however, the details of the tests reported here pertain only to the uniaxial tests in the truly triaxial device to determine their orthotropic constants.

Stress Path Dependency

Figure 3 shows the various stress paths and their directions in the principal stress space. Hydrostatic compression (HC), conventional triaxial compression (CTC), conventional triaxial extension (CTE), reduced triaxial compression (RTC), and reduced triaxial extension (RTE) paths lie in the triaxial plane. Triaxial compression (TC), triaxial extension (TE), and simple shear (SS) paths lie in the octahedral plane. All these stress paths can be simulated easily in the truly triaxial device.

Analysis of Test Results

Tests along each stress path other than HC are repeated a number of times either with different confining pressures (CTC, CTE), with different values of octahedral stress [σ_{oct} (SS, TC, TE)], or with different values of major principal stress [σ_1 (RTC, RTE)]. The stress-strain responses in terms of axial strain and lateral strains are plotted against mean normal stress for the HC path; against deviatoric stress for the CTC, CTE, RTC, and RTE paths; and against octahedral shear stress for SS, TC, and TE paths.

In case of the ballast, both kinds of scaled-down materials are tested to investigate the grain size effect on strength and deformation characteristics; details are not reported here. The volumetric (hydrostatic) behavior of the material is not affected significantly by particle size. The scaled-down model material, with a mean particle size of 0.63 in., is tested with different stress paths and the material model is developed based on those test results (11).

For the determination of orthotropic elastic constants, the uniaxial tests should be conducted along the three principal directions of the material; namely, longitudinal (L), radial (R), and tangential (T) directions (12,13) (Figure 4). Wood samples are tested for uniaxial compression; however, deformations are recorded in all three directions. Within the elastic limit the same sample can be tested in all three directions, one after the other. Furthermore, the high-capacity, truly triaxial device enables the uniaxial tests to be performed on the same sample along the three (L, R, and T) directions without retrieving the sample.

This device is only capable of applying normal stresses (to find the elastic shear constants); therefore, the technique used is to cut a specimen with an oblique orientation of 45 degrees (Figure 5) with respect to its principal material planes, test it, and then resolve the applied normal stresses into components of shear and normal stresses on those principal planes (6,13). The nine orthotropic constants are then evaluated.

CONSTITUTIVE LAWS

The stress-strain responses of the materials observed in this investigation are used to develop constitutive models for the four materials. A few typical stress-strain response curves are presented here: HC test for ballast (Figure 6); CTC test for subballast (Figure 7); SS test for subgrade soil (Figure 8); uniaxial test on wood with $\alpha = 0$ degrees (Figure 9); and uniaxial test on wood with $\alpha = 45$ degrees (Figure 10).

A critical-state material model appears to fit the behavior of the subgrade soil. A cap model appears to fit the behavior of the subballast. Resilient modulus and variable moduli models are developed for the ballast. Orthotropic elastic law is defined for wood. Details of the models developed and the model parameters determined are given in the following paragraphs.

Figure 4. Orthotropic wood.

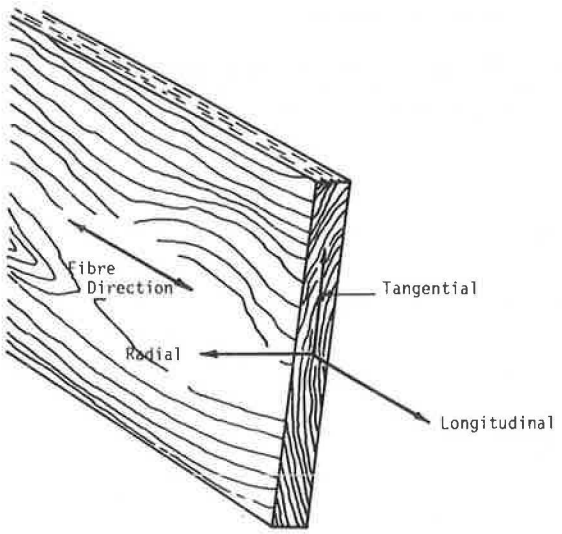

Subgrade Soil

A critical-state model (14,15) can be used to characterize the constitutive behavior of the soil. The two parameters λ and κ, the constants related to compression and swelling parts of e-ln p curves, are found to be 0.017 and 0.0028, respectively. To find the failure surface the straight-line stress paths followed are plotted in J_1, $\sqrt{J_{2D}}$ space, where J_1 is the first invariant of stress tensor and J_{2D} is the second invariant of deviator stress tensor. The failure stress for a given curve is adopted as the asymptotic value in the ultimate range of the behavior. The failure surface is then drawn through the points of average failure stress levels as marked along the respective stress paths (Figure 11). The slope of this line in J_1 versus $\sqrt{J_{2D}}$ space is 0.286 and the yield function (F) for the modified cam clay model (14) is

$$F = q^2 - (1.48)^2 p_0 p + (1.48)^2 p^2 = 0 \quad (1)$$

where

p = normal stress,
q = deviator stress,
p_0 = mean normal stress, and
M = slope of critical-state line (= 1.48).

Figure 5. Oriented cube with $\alpha = 45°$.

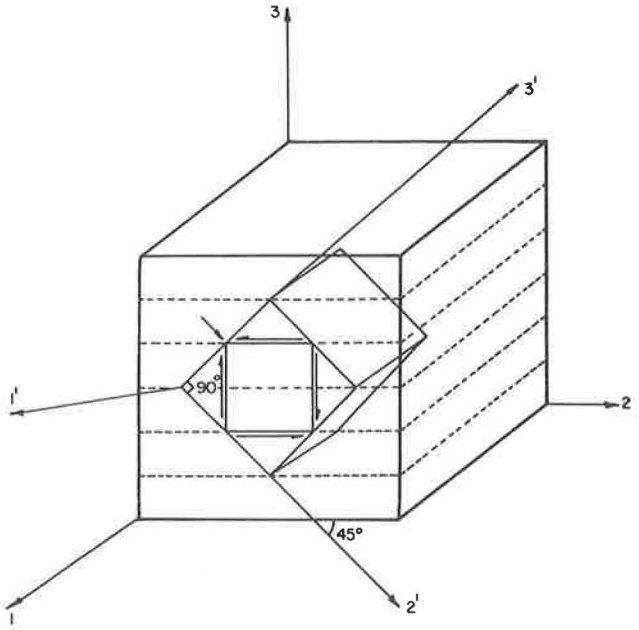

Subballast

The stress-strain response of this material indicates that it undergoes both elastic and plastic strains from the start of the loading. An elastic-plastic hardening cap model (16) is adopted for subballast.

The failure envelope fitted to this material is a combination of Drucker-Prager (17) and von Mises failure surfaces; the former for low levels of stress (J_1) and the latter for high levels of stress. Both are connected by an exponential transition surface (6,18). The surface is defined as

$$\sqrt{J_{2D}} = \alpha + \beta J_1 - \gamma \exp^{-J_1 \theta} \quad (2)$$

where the parameters α, β, γ, and θ are evaluated from the fitted failure surface as α is 26.4 psi, β is 0.18, γ is 21.5 psi, and θ is -0.0003. At high levels of stress the von Mises surface is

$$F = \sqrt{J_{2D}} - k_1 = 0 \quad (3)$$

where k_1 is found to be 26.4 psi.

The plastic potential and yield surfaces are drawn by sketching on J_1 versus $\sqrt{J_{2D}}$ curves orthogonal to the plastic strain increment vectors (Figure 12) and the yield surfaces are plotted as

Figure 6. Stress-strain response curves for hydrostatic compression test, ballast.

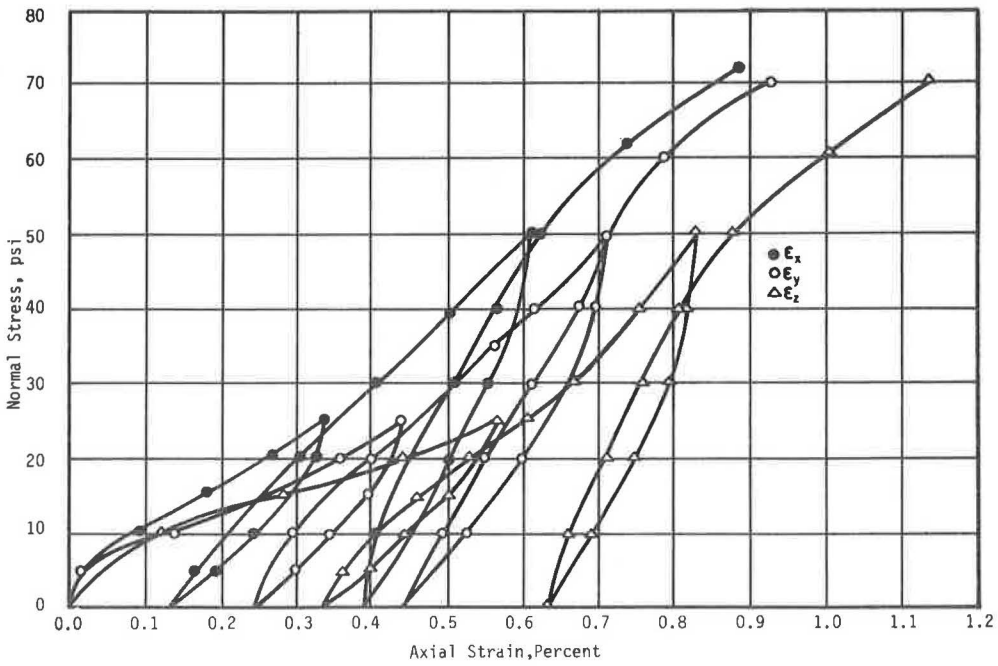

Figure 7. Stress-strain response curves for conventional triaxial compression test, subballast (σ_3 = 25.00 psi).

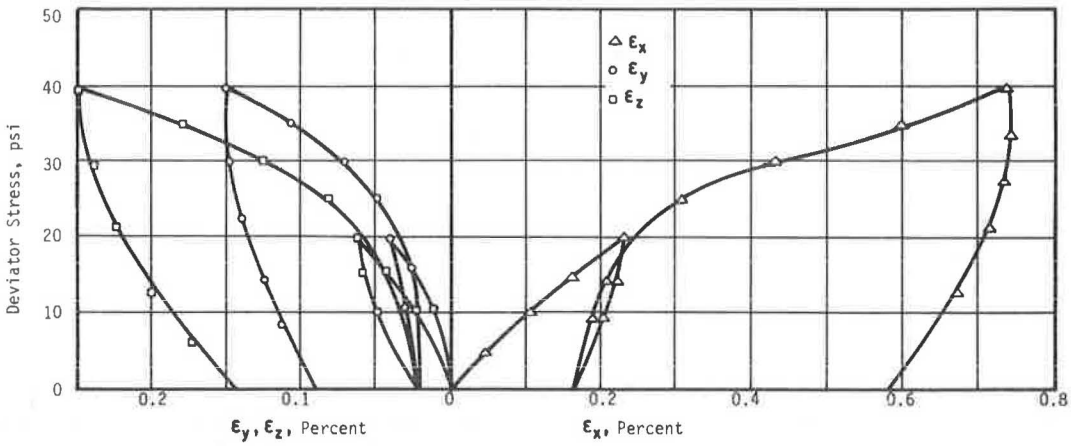

Figure 8. Stress-strain response curves for simple shear test, soil.

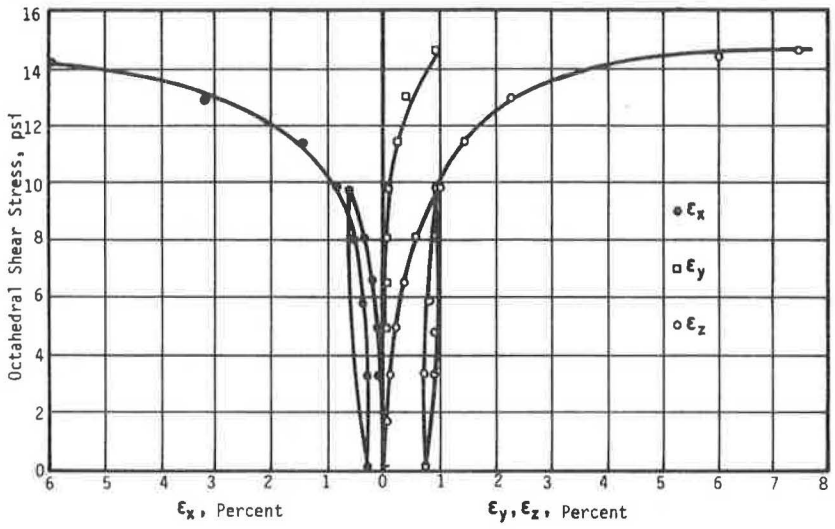

Figure 9. Stress-strain response curves for uniaxial compression test, wood (α = 0 degrees).

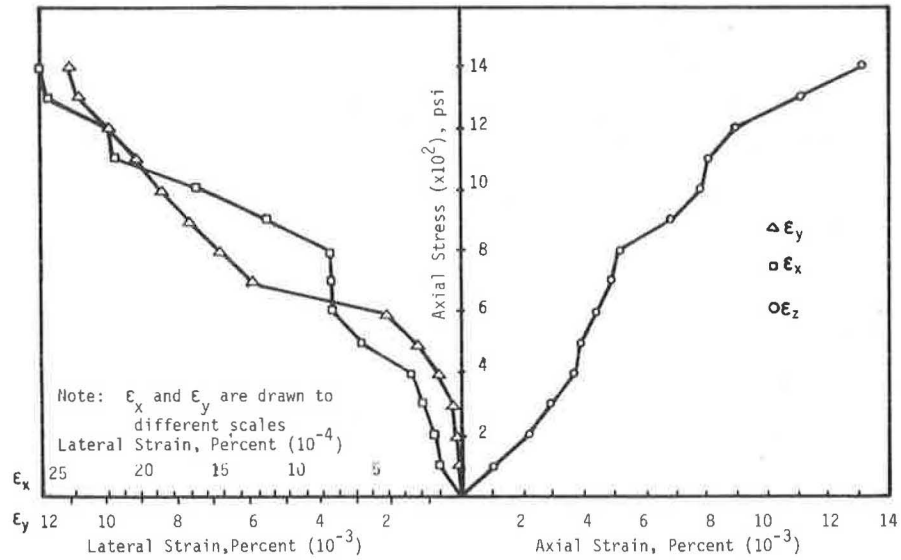

Figure 10. Stress-strain response curves for uniaxial compression test, wood (α = 45 degrees).

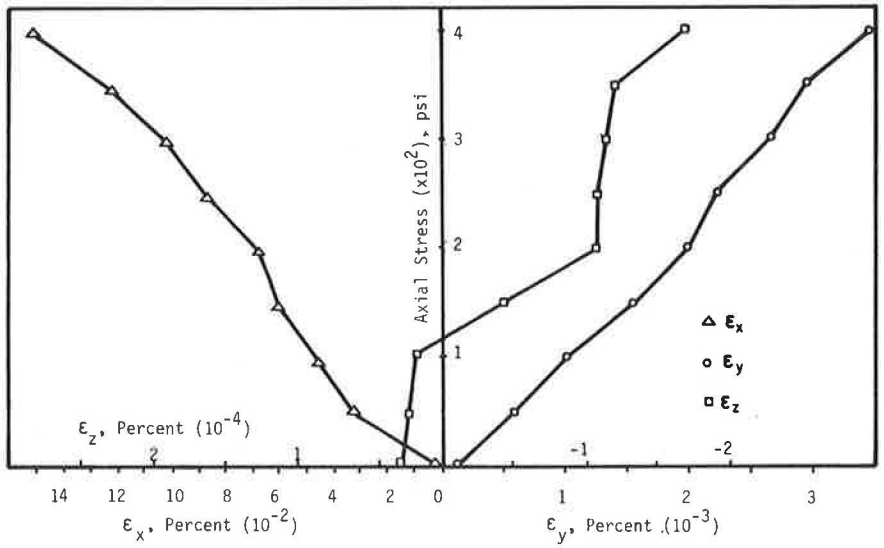

Figure 11. Failure envelope for subgrade soil.

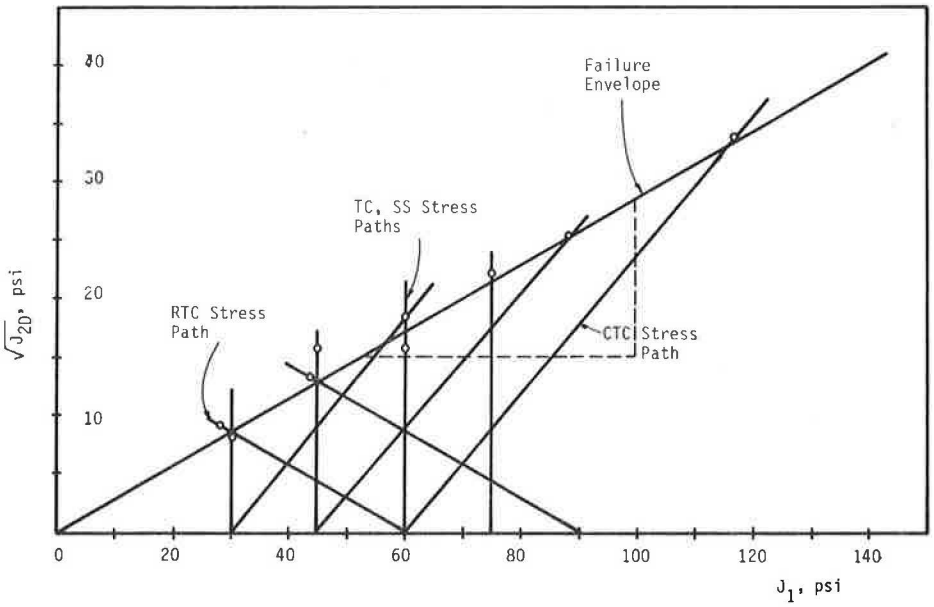

Figure 12. Plastic strain increment vectors and potential surfaces.

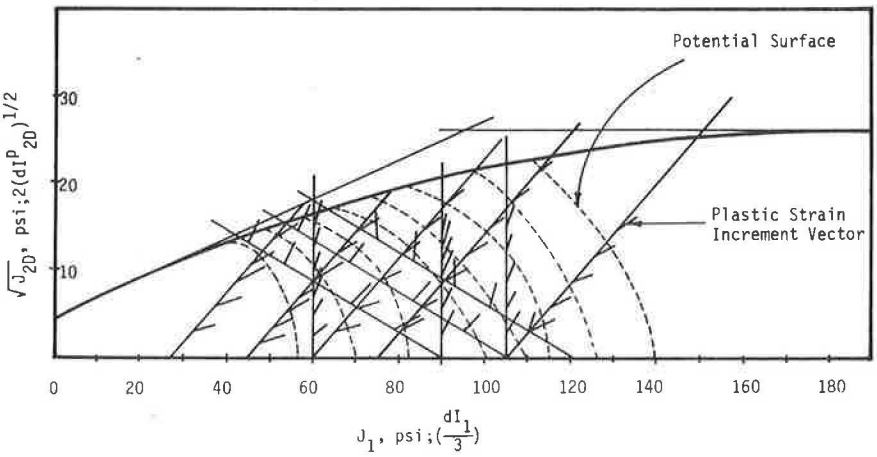

Figure 13. Yield surfaces.

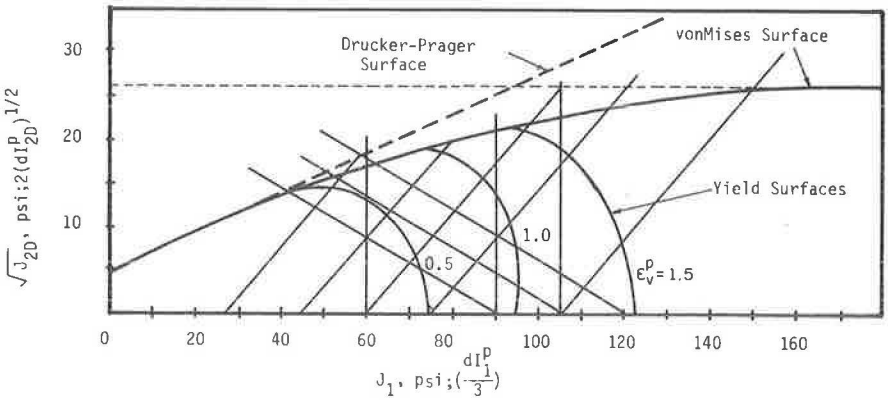

equal contours of volumetric plastic strains (Figure 13). The yield surface (Figure 13) is found nearly elliptical in shape and can be expressed as (16)

$$R^2 J_{2D} + (J_1 - L)^2 - R^2 b^2 = 0 \quad (4)$$

where R is the ratio between the principal axes of the ellipse and b is the $\sqrt{J_{2D}}$ value when J_1 equals L, L equals the J_1 value at the center of ellipse, and Rb equals X-L where X is the J_1 value at the intersection between the ellipse and J_1 axis. Here R is found to be about 1.20.

The potential and yield surfaces are not the same, which leads to a conclusion that the material exhibits nonassociative characteristics. A simple approach to incorporate the nonassociative behavior can be used; this approach is described elsewhere (15,19).

Ballast

The test results are used to develop two types of constitutive models, (a) resilient modelus and (b) variable moduli. The resilient modulus approach allows consideration of ballast as nonlinear elastic material. The resilient modulus (20-22) as determined from various test results that have different confining pressures is found to be

$$E = 1{,}300\,\bar{\sigma}_3^{0.87} \quad (5)$$

where E is the resilient modulus (psi) and $\bar{\sigma}_3$ is the effective confining pressure (psi).

Note, however, that the ballast exhibits inelastic or plastic behavior. The variable moduli model, therefore, is proposed to allow approximately for the inelastic behavior. In the combined stress-strain variable moduli model both the shear modulus and bulk modulus are assumed to depend on the stress and strain invariants (23). They can be expressed as

$$K = K_0 + K_1 I_1 + K_2 I_1^2 \quad (6)$$

$$G = G_0 + \gamma_1 J_1 + \gamma_2 J_{2D}^{0.5} \quad (7)$$

where

I_1 = first invariant of strain tensor,
K_0 = initial bulk modulus,
G_0 = initial shear modulus, and
K_1, K_2, γ_1, and γ_2 = material parameters.

The parameters are determined by the process of curve fitting on the laboratory test data:

$$K_0 = 4.00 \times 10^3 \text{ psi} \quad (8a)$$

$$G_0 = 1.71 \times 10^3 \text{ psi} \quad (8b)$$

$$\gamma_1 = 2.59 \quad (8c)$$

$$\gamma_2 = -60.17 \quad (8d)$$

$$K_1 = -5.49 \times 10^5 \quad (8e)$$

$$K_2 = 2.54 \times 10^7 \text{ psi} \quad (8f)$$

Relations similar to those in Equations 6 and 7 can be used to define unloading and reloading moduli. It may often be appropriate to adapt them to be equal to or multiples of the initial moduli (K_0 and G_0) (11,15). The foregoing model is found satisfactory to reproduce actual ballast behavior under triaxial stress states.

Wood

The constitutive equation for wood as an orthotropic elastic body may be written in matrix form as (24)

$$\begin{Bmatrix} \epsilon_{11} \\ \epsilon_{22} \\ \epsilon_{33} \\ \epsilon_{12} \\ \epsilon_{23} \\ \epsilon_{31} \end{Bmatrix} = \begin{bmatrix} \frac{1}{E_{11}} & \frac{-\nu_{21}}{E_{22}} & \frac{-\nu_{31}}{E_{33}} & & & \\ \frac{-\nu_{12}}{E_{11}} & \frac{1}{E_{22}} & \frac{-\nu_{32}}{E_{33}} & & [0] & \\ \frac{-\nu_{13}}{E_{11}} & \frac{-\nu_{23}}{E_{22}} & \frac{1}{E_{33}} & & & \\ & & & \frac{1}{G_{23}} & & \\ & [0] & & & \frac{1}{G_{13}} & \\ & & & & & \frac{1}{G_{12}} \end{bmatrix} \begin{Bmatrix} \sigma_{11} \\ \sigma_{22} \\ \sigma_{33} \\ \sigma_{12} \\ \sigma_{23} \\ \sigma_{31} \end{Bmatrix} \quad (9)$$

The nine independent orthotropic elastic parameters E_{11}, E_{22}, E_{33}, G_{12}, G_{13}, G_{32}, ν_{12}, ν_{13}, and ν_{32} are determined from the uniaxial compression test results. The results of three uniaxial compression tests conducted with α equal to 0 and the loading axis in the longitudinal radial and tangential directions are used to find E and ν. The shear parameters (G) are determined from the results of the uniaxial compression tests on 45-degree, obliquely oriented cubes. The orthotropic elastic constants determined are given below.

For Young's modulus,

E_{11} = 22.03 x 10^5 psi, E_{22} = 20.34 x 10^4 psi, and E_{33} = 18.68 x 10^4 psi.

For shear modulus,

G_{13} = 19.61 x 10^4 psi, G_{12} = 13.44 x 10^4 psi, and G_{23} = 46.15 x 10^3 psi.

Poisson's ratios are

ν_{12} = 0.215, ν_{13} = 0.347, ν_{21} = 0.241, ν_{23} = 0.221, ν_{32} = 0.324, and ν_{31} = 0.302.

CONCLUSIONS

Results from a comprehensive series of tests on materials from rail-track support structures tested in truly triaxial testing devices are discussed. A number of factors such as stress path and state of stress are included in the testing and modeling programs.

The subgrade soil under this study exhibits nonlinear, inelastic, dilatant, and strain-hardening behavior. A critical-state material model (modified cam clay model) is adopted for this material. An elastoplastic, isotropic hardening material model (cap model) is used for the subballast. Ballast undergoes both elastic and plastic strains from the start of the loading. The volumetric (hydrostatic) behavior of the material is affected significantly by the grain size; however, the resilient modulus is dependent on particle size and so also is the shear behavior of the material. A variable moduli model is used for ballast, as an alternative to the resilient modulus approach, to account for its elastic-plastic behavioral response. The stress-strain response of wood, even in uniaxial testing, is observed to be nonlinear. The elastic parameters based on orthotropic behavior are determined from the test results.

The foregoing models appear to provide satisfactory representations for the four track materials. They have been verified by comparing predictions with the laboratory test data. Furthermore, the models were implemented in two- and three-dimensional finite-element procedures (7,25). Here, the finite-element predictions were compared with observations of stresses and displacements at various test sections at TTC, including those at the UMTA section. Details of these verifications are given elsewhere (8).

The modeling and prediction capability of (numerical) solution procedures for track structures can be improved if the behavior of the component materials is found from (three-dimensional) tests that simulate the field conditions.

ACKNOWLEDGMENT

The research results presented herein were obtained under contract from the Office of University Research, U.S. Department of Transportation.

REFERENCES

1. G.P. Raymond et al. Repeated Load Triaxial Tests on a Dolomite Ballast. Journal of the Geotechnical Engineering Division, ASCE, No. GT7, 1978.
2. C.A. Burdell. State-of-the-Art of USA Railroad Cross Ties. Report to the Railway Tie Assn., Aug. 1977.
3. E.T. Selig and A. Slurz. Ballast and Subgrade Response to Train Loads. TRB, Transportation Research Record 694, 1978, pp. 53-60.
4. C.S. Desai, R. Janardhanam, and S. Sture. High Capacity Truly Triaxial Device and Its Applications. Journal of Geotechnical Testing, AASTM, March 1982.
5. S. Sture and C.S. Desai. Fluid Cushion Truly Triaxial or Multiaxial Testing Device. Journal of Geotechnical Testing, ASTM, Vol. 2, No. 1, 1979.
6. R. Janardhanam. Constitutive Laws of Materials in Track Support Structures. Virginia Polytechnic Institute and State Univ., Blacksburg, Ph.D. Dissertation, 1981.
7. H.J. Siriwardane. Nonlinear Soil-Structure Interaction Analysis of One-, Two- and Three-Dimensional Problems Using Finite Element Method. Virginia Polytechnic Institute and State Univ., Blacksburg, Ph.D. Dissertation, Nov. 1980.
8. C.S. Desai, H.J. Siriwardane, and R. Janardhanam. Interaction and Load Transfer Through Track Support Systems--Part 1: One-, Two- and Three-Dimensional Nonlinear Soil-Structure Interaction, Finite Element Procedures and Verification. U.S. Department of Transportation, Rept. DPT/RSPA/DMA-50/83/11, 1983.
9. C.S. Desai, H.J. Siriwardane, and R. Janardhanam. Interaction and Load Transfer Through Track Support Systems--Part 2: Testing and Modelling of Materials and Interfaces. U.S. Department of Transportation, Rept. DOT/RSPA DMA-50/83/11, 1983.
10. J. Lowe. Shear Strength of Coarse Embankment Dam Materials. Proc., 8th Congress of Large Dams, International Commission for Large Dams, Paris, 1964.
11. R. Janardhanam and C.S. Desai. Three-Dimensional Testing and Modelling of a Ballast. Journal of the Geotechnical Engineering Division, ASCE, Vol. 108, No. GT6, June 1983.
12. J. Bodig and J.R. Goodman. Prediction of Elastic Parameters for Wood. Wood Science, Vol. 5, No. 4, 1973.
13. J.R. Goodman and J. Bodig. Orthotropic Elastic Properties of Wood. Journal of the Structural Engineering Division, ASCE, Vol. 96, No. ST11, 1970.
14. K.H. Roscoe and J.B. Burland. On the Generalized Stress-Strain Behavior of "Wet" Clay. In Engineering Plasticity (J. Hegman and F.A. Leckie, eds.), Cambridge Univ. Press, Cambridge, United Kingdom, 1968, pp. 535-609.
15. C.S. Desai and H.J. Siriwardane. Constitutive Laws for Engineering Materials: With Emphasis on Geologic Materials. Prentice-Hall, Englewood Cliffs, N.J., 1984.
16. F.L. DiMaggio and I.S. Sandler. Material Model for Granular Soils. Journal of the Engineering Mechanics Division, ASCE, Vol. 197, No. 3, 1971.
17. D.C. Drucker. Some Implications of Work-Hardening and Ideal Elasticity. Quarterly of Applied Mathematics, Vol. 7, No. 4, 1950.
18. S. Sture, C.S. Desai, and R. Janardhanam. Development of a Constitutive Law for an Artificial Soil. Proc., 3rd International Conference on Numerical Methods in Geomechanics, Aachen, West Germany, 1979.
19. C.S. Desai and M.O. Faruque. A Generalized Basis for Modelling Plastic Behavior of Materials. Proc., International Conference on Constitutive Laws of Engineering Materials. Univ. of Arizona, Tucson, Jan. 1983.
20. R.D. Barksdale. Repeated Load Test Evaluation of Base Course Materials. Georgia Institute of Technology, Atlanta, Ph.D. Thesis, 1972.
21. J.J. Allen and M.R. Thompson. Resilient Response of Granular Materials Subjected to Time

Dependent Lateral Stress. TRB, Transportation Research Record 510, 1974, pp. 1-13.
22. J.R. Boyce, S.F. Brown, and P.S. Pell. The Resilient Behaviour of a Granular Material Under Repeated Loading. Proc., Australian Road Research Board, Vol. 8, 1976, pp. 1-12.
23. I. Nelson and M.L. Baron. Investigation of Ground Shock Effects on Nonlinear Hysteretic Media. Defense Nuclear Agency, Washington, D.C., Repts. 1 and 2, 1969.
24. I.S. Sokolnikoff. Mathematical Theory of Elasticity. McGraw-Hill, New York, 1956.
25. C.S. Desai and H.J. Siriwardane. Numerical Models for Track Support Structures. Journal of the Geotechnical Engineering Division, ASCE, Vol. 108, No. GT3, March 1982.

Publication of this paper sponsored by Committee on Track Structure System Design.

Innovations in Track Structures on Long Island Rail Road—Rationale, Design Criteria, and Performance

MOHAMMAD S. LONGI

During the last 20 to 25 years, the Long Island Rail Road (LIRR) has designed or participated in the design and construction of various grade elimination projects. The earlier projects (1958-1970) entailed embankment sections with conventional track structure—wood ties, jointed rail, and ballast. The viaduct sections were cast-in-place, reinforced concrete deck with ballast, wood ties, and jointed rail. Since 1970 LIRR has embarked on various innovative track structures and their associated components, which entailed continuous welded rail, elastic fastener clips, direct fixation fastening system, and concrete slab track. Some of the considerations in selection of the new design features were availability of technology, improved ride quality, faster operating speeds, and reduced maintenance costs. Various improved track structures are discussed in this paper and the rationale, design criterion, field measurements, findings, and performance are described.

Between 1912 and 1916 concrete slabs were installed on three separate occasions on soft roadbed for the support of ordinary ballasted track. These installations were

1. Under main line crossovers in Jamaica,
2. Under main tracks on a 20-ft fill behind bridge abutments, and
3. On a silt fill at the rear of a bulkhead for loading car ferries.

The first installation entailed 73,000 ft² of cast-in-place concrete subballast slabs under 49 turnouts in the Jamaica Interlocking (1). Concrete slabs were 8-in. thick and unreinforced. A few years after construction a cave-in occurred under one of the slabs. The supporting slab held the ballast and track intact, and the traffic was only delayed slightly. After nearly 70 years of passenger and freight traffic, these installations are still performing satisfactorily.

PROJECT CORRIDOR

The Babylon branch on the Long Island Rail Road (LIRR) is the busiest. Every day it carries 33,452 commuters in the morning (6:00 to 10:00 a.m.) and 27,426 commuters in the afternoon (4:00 to 7:00 p.m.) and employs 148 commuter (revenue) trains. The average train speed is 60 mph and the maximum speed is 80 mph. The 40-mile trip from Babylon to Pennsylvania Station, central business district (CBD) of New York City, takes 53 min (minimum) travel time. Twenty-five percent of the daily commuter traffic is on this corridor. Some freight traffic also uses this branch. Traffic is estimated at approximately 12 million tons per year. During the last 20 to 25 years the various sections of this route have been elevated, thus eliminating the accident hazard at the grade crossings between trains and vehicular traffic. The elevated structures are either earth embankments, simple span concrete viaducts, or individual bridges.

The various rail improvement projects constructed during the last 25 years are presented in this paper. The track structure elements of these projects will be emphasized. The focus is on the evolution of track structures in these projects. First conventional wood tie ballast was used, followed by direct fixation track, and finally concrete slab track structures were used.

CONVENTIONAL TRACK STRUCTURES

From 1958 through 1970, LIRR was involved in various rail improvement projects. Nearly 20 miles of double tracking was constructed on the Babylon corridor as part of grade elimination projects. The projects included elevation of railroad tracks in Nassau and Suffolk Counties of New York.

Embankment Sections

Embankment sections were an average of 17- to 20-ft high. Track structures were comprised of 12-in. standard ballast section. Wooden ties (7 in. x 9 in. x 8 ft 6 in.) at 21.25 in. center to center. The running rail weighed 115-lb in 39-ft lengths. The ends of the rail sections being joined by means of joint bars and bolts thus formed an expandable joint. The rails were attached to the wooden ties by cut spikes driven through holes in tie plates that were inserted between the base of the rail and the top of the tie. Figure 1 shows a typical wood tie track.

Concrete Viaducts

Concrete viaducts were either cast-in-place deck or prestressed beams with poured-in-place composite concrete decking. Track structure was composed of 115-lb running rail (39-ft sections fastened with